



# INVESTIGATION OF ALTERNATIVE RETURN STRATEGIES FOR ORION TRANS-EARTH INJECTION DESIGN OPTIONS

Belinda G. Marchand and Sara K. Scarritt  
The University of Texas at Austin

Thomas A. Pavlak and Kathleen C. Howell  
Purdue University

Michael W. Weeks  
NASA Johnson Space Center





# Autonomous Targeting Goals

- LLO → EEI via 3 Deterministic  $\Delta V$ 's
  - EEI Targets: ALT, FPA & AZ, LAT & LON
  - Controls: Up to 3 Deterministic  $\Delta V$ 's
  - Feasible Total  $\Delta V < 1.5$  km/sec
  - Turn-key return capability required
- Targeting in Sun perturbed Earth-Moon 3BP
  - N-body regimes (for  $N > 2$ ) → Iterative Solution Process
  - Feasible or Optimal Algorithms Require Startup Arc
  - Quality of startup arc is crucial for onboard determination
    - 2BP vs 3BP Startup Arcs



# Precision Earth Entry from Polar LLO

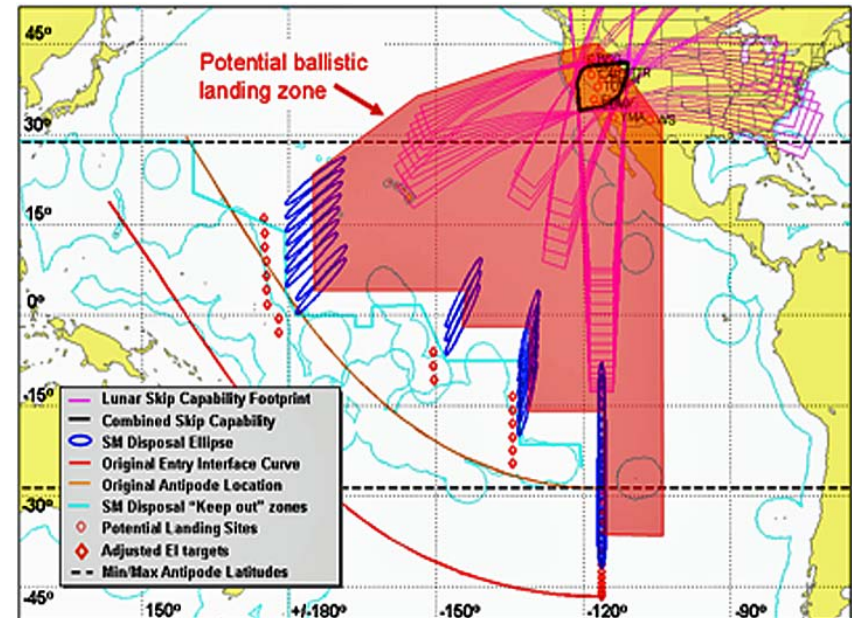
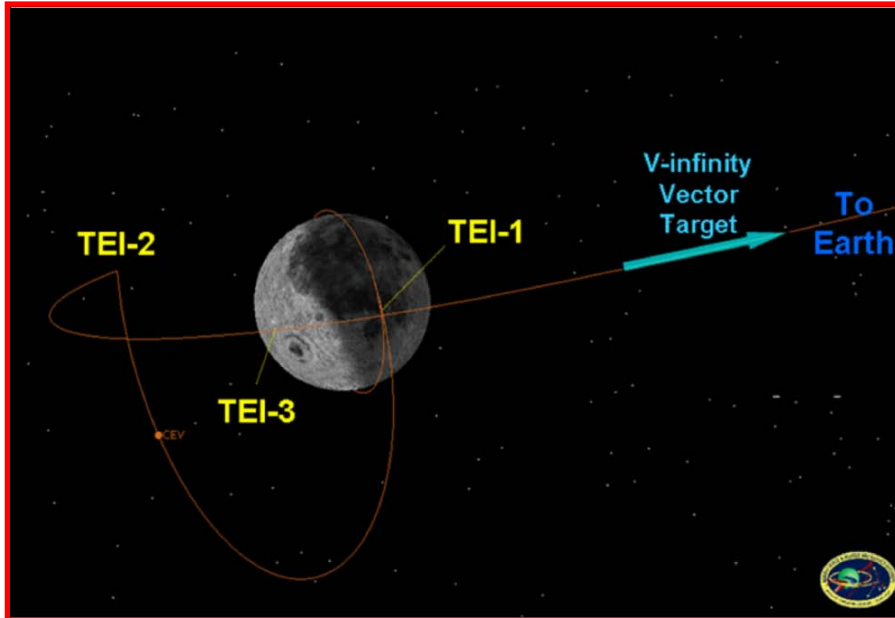
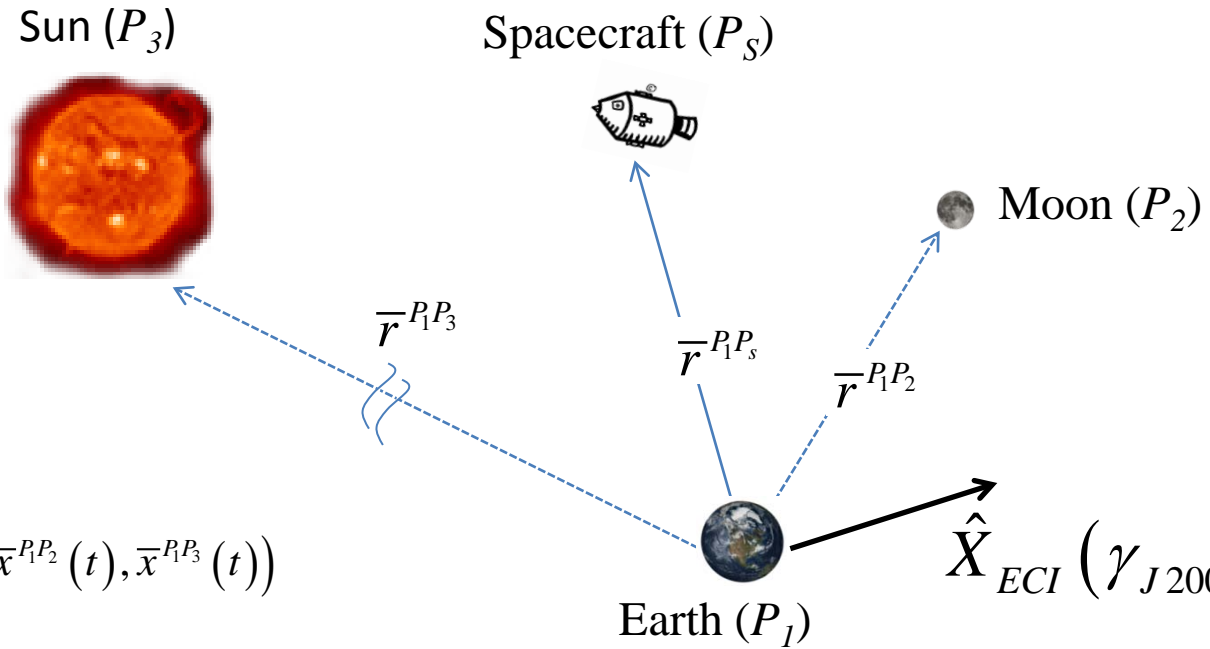


Table 1. Entry Interface Parameters

Entry Parameter	EI-1	EI-2	EI-3	EI-4	EI-5	EI-6
Longitude	-115.5°	-121.00°	-134.5456°	-151.4038°	173.5216°	175.6365°
Latitude	-46.66992°	-8.8522°	-19.20410°	-7.14720°	15.36700°	15.36700°
Flight Path Azimuth	0.0°	0.0°	13.9960°	34.1065°	62.3311°	49.3291°
Flight Path Angle	-5.81°	-5.99°	-6.03°	-6.16°	-6.16°	-5.86°



# Ephemeris (EPHEM) Model: Sun Perturbed Earth-Moon System



$$\bar{x}^{P_1 P_s} = \begin{bmatrix} \bar{r}^{P_1 P_s} \\ ECI \dot{\bar{r}}^{P_1 P_s} \end{bmatrix}$$

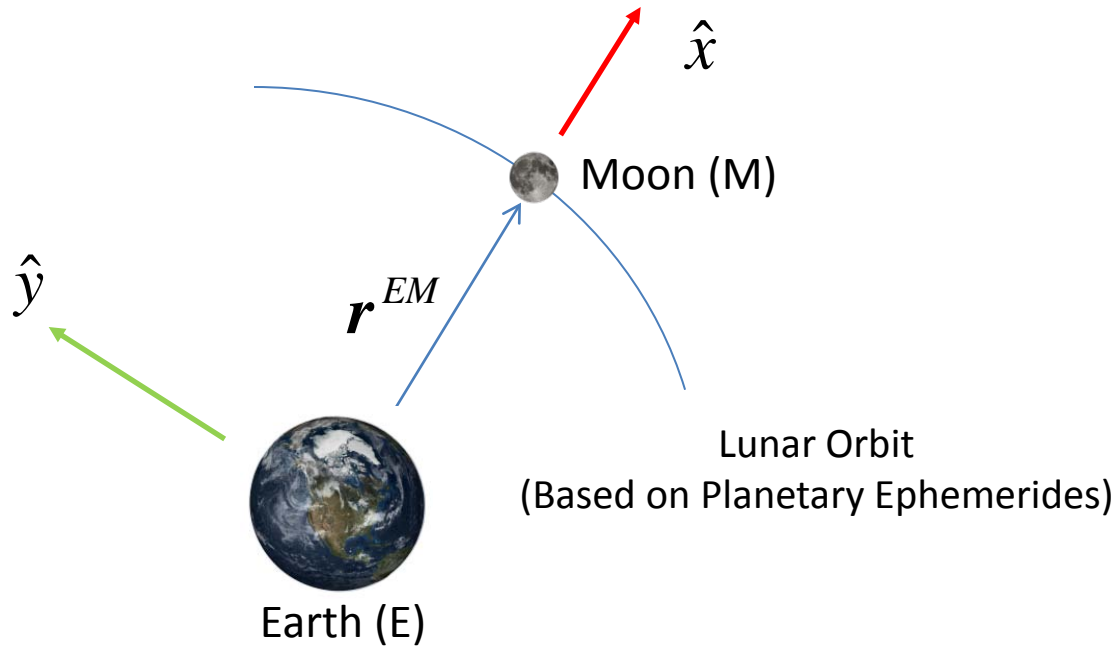
$$ECI \dot{\bar{x}}^{P_1 P_s} = \begin{bmatrix} ECI \dot{\bar{r}}^{P_1 P_s} \\ ECI \ddot{\bar{r}}^{P_1 P_s} \end{bmatrix} = \bar{f}(t, \bar{x}^{P_1 P_s}(t), \bar{x}^{P_1 P_2}(t), \bar{x}^{P_1 P_3}(t))$$

$$\bar{f}(t, \bar{x}^{P_1 P_s}(t), \bar{x}^{P_1 P_2}(t), \bar{x}^{P_1 P_3}(t)) = -\frac{\mu_{P_1}}{\|\bar{r}^{P_1 P_s}(t)\|^3} - \sum_{j=2}^3 \mu_{P_j} \left( \frac{\bar{r}^{P_1 P_s}(t) - \bar{r}^{P_1 P_j}(t)}{\|\bar{r}^{P_1 P_s}(t) - \bar{r}^{P_1 P_j}(t)\|^3} + \frac{\bar{r}^{P_1 P_j}(t)}{\|\bar{r}^{P_1 P_j}(t)\|^3} \right)$$

$\bar{r}^{P_1 P_2}(t), \bar{r}^{P_1 P_3}(t) \Rightarrow$  From JPL DE405 Ephemerides



# The Synodic Rotating Frame (SRF)



$$\hat{\mathbf{x}} = \frac{\mathbf{r}_{ECI}^{EM}}{\|\mathbf{r}_{ECI}^{EM}\|}$$

$$\hat{\mathbf{z}} = \frac{\mathbf{r}_{ECI}^{EM} \times \mathbf{v}_{ECI}^{EM}}{\|\mathbf{r}_{ECI}^{EM} \times \mathbf{v}_{ECI}^{EM}\|}$$

$$\hat{\mathbf{y}} = \hat{\mathbf{z}} \times \hat{\mathbf{x}}$$

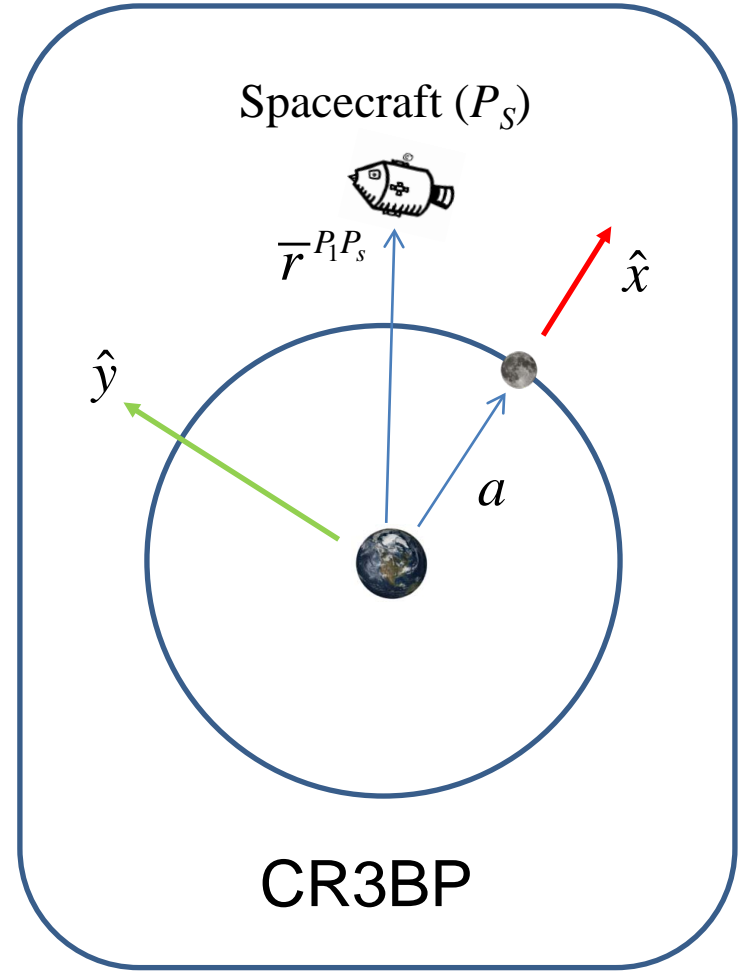
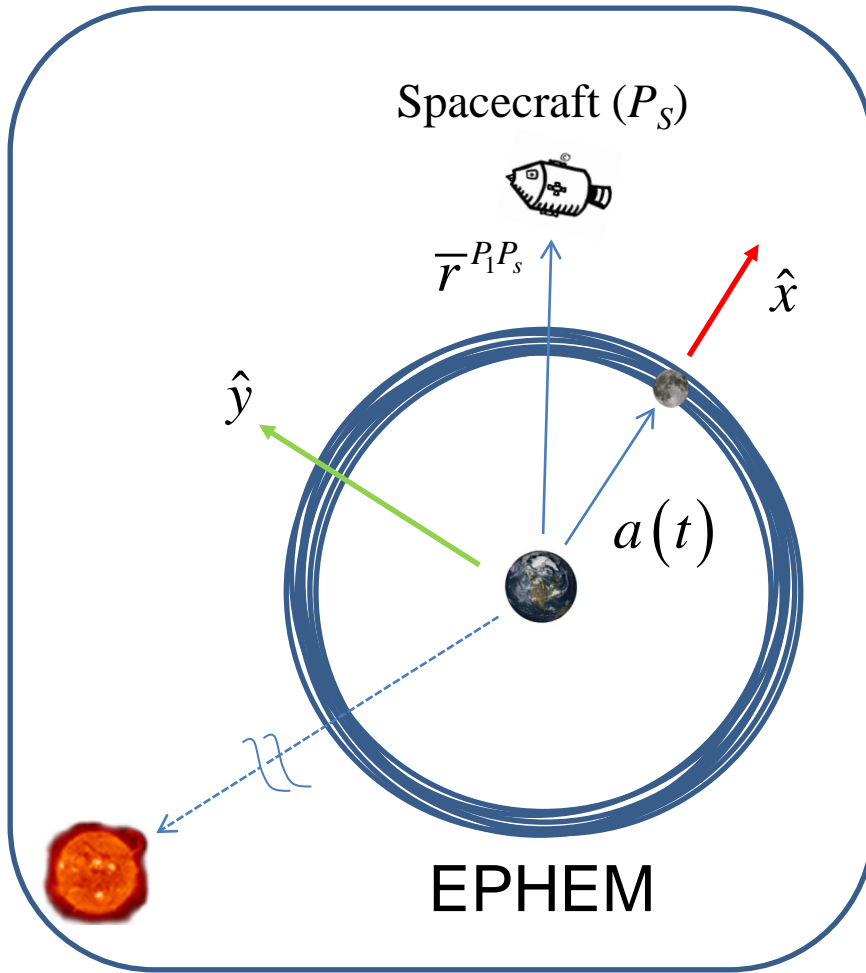
ECI = Earth Centered Inertial Frame (EME J2000)

SRF = Synodic Rotating Frame

$${}^{ECI}C^{SRF} = \begin{bmatrix} \hat{\mathbf{x}} & \hat{\mathbf{y}} & \hat{\mathbf{z}} \end{bmatrix} \longrightarrow \mathbf{r}_{SRF}^{ES} = [{}^{ECI}C^{SRF}]^T \mathbf{r}_{ECI}^{ES}$$

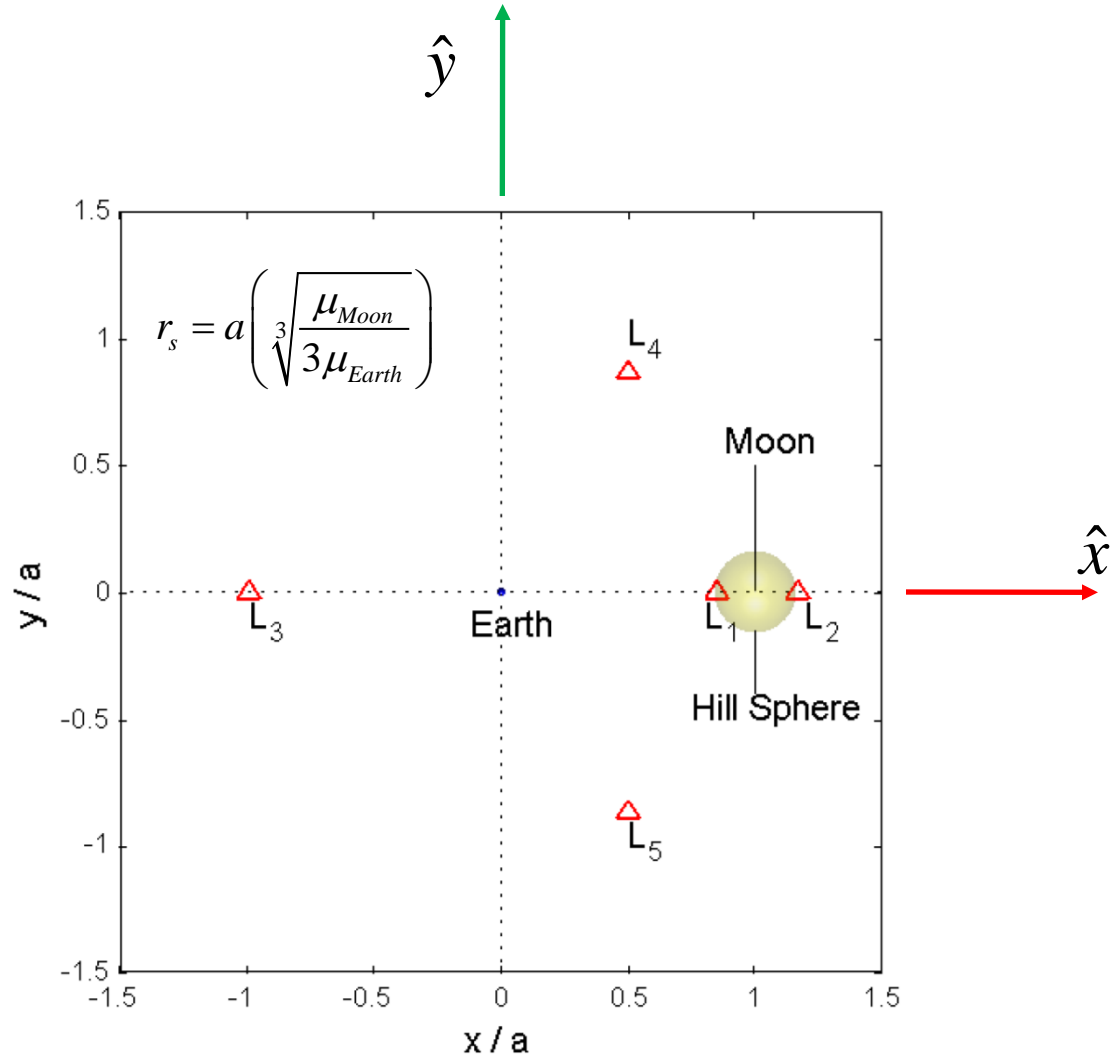


# Ephemeris Model vs. The Circular Restricted 3-Body Problem





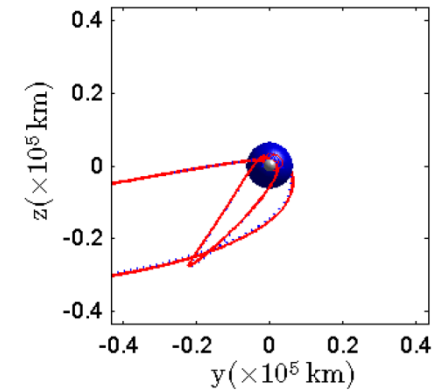
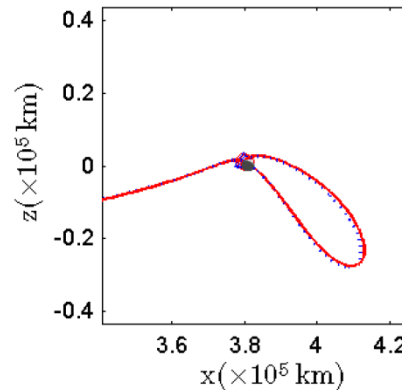
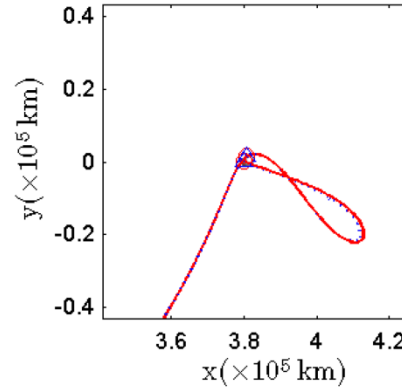
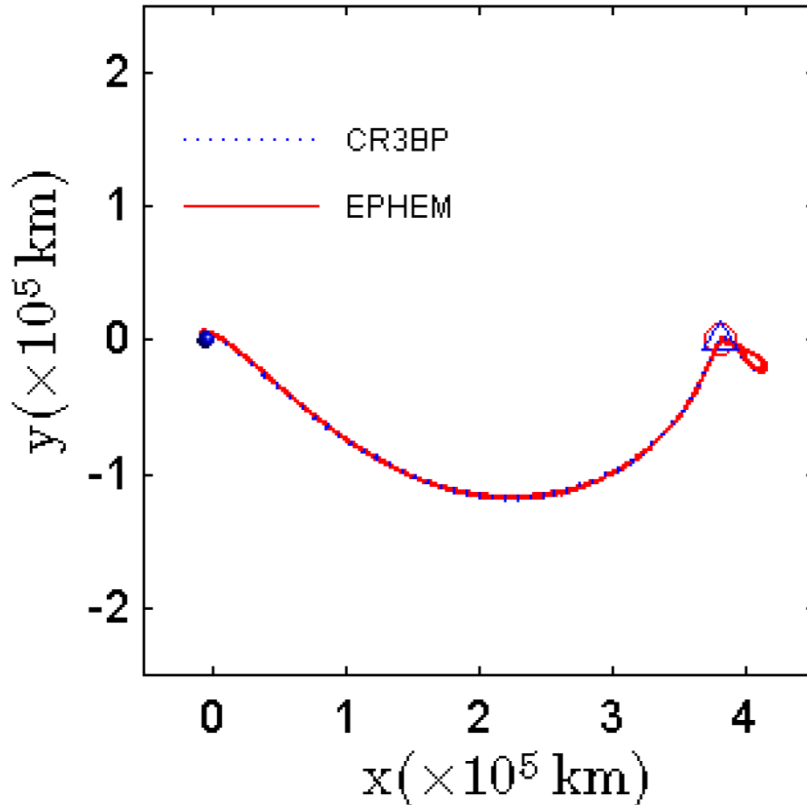
# The Hill Sphere in the Earth-Moon CR3BP





# Comparison of Moon-to-Earth Transfers: CR3BP vs. EPHEM Models

Targets: **Altitude = 121.912 km**, **FPA = -5.86 deg**,  $\Delta V = 1.0$  kps



Close-up View Near the Moon:  
(SRF View)





# Assessing Entry Constraint Coupling and it's Impact on Startup Arc Selection

- For each **Earth Entry Interface** (EEI-k, for k=1,...,6) State
  1.  $U_k$  = set of sample perturbed states relative to EEI-k
  2.  $W_k$  = set of trajectories generated by

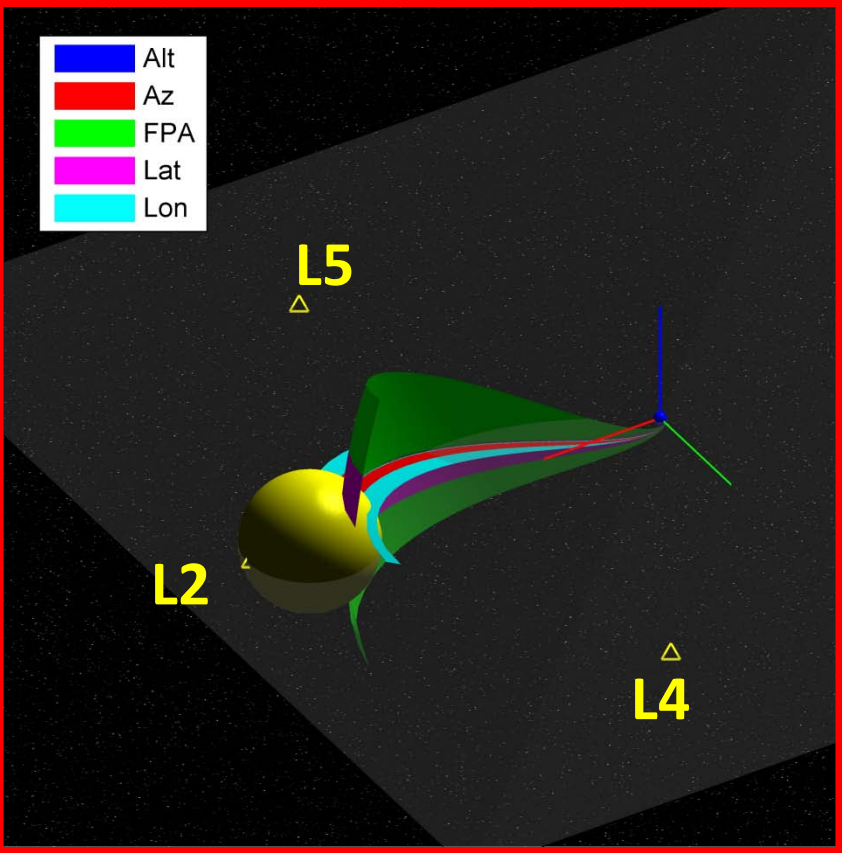
$$\bar{x}^{P_1 P_s}(t) = \bar{x}^{P_1 P_s}(t_{EEI}) + \int_{t_{EEI}}^t \bar{f}(\tau, \bar{x}^{P_1 P_s}(\tau), \bar{x}^{P_1 P_2}(\tau), \bar{x}^{P_1 P_3}(\tau)) d\tau$$

$W_k$  forms the **dispersion manifold** for EEI-k.

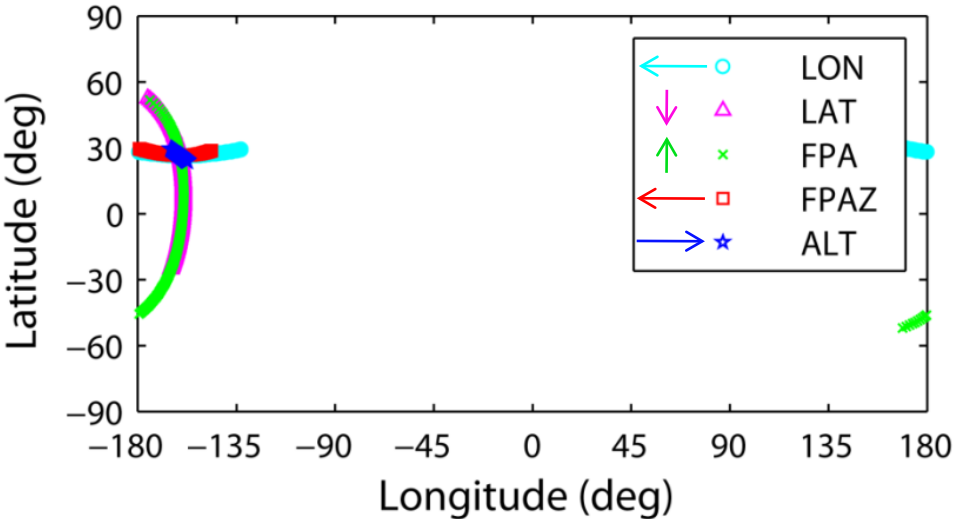
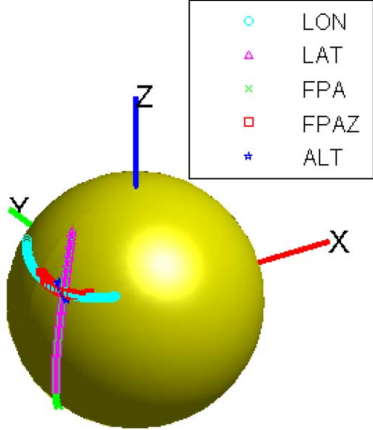
3.  $\Omega_k = [^{SRF}C^{ECI}] W_k$
4.  $\Omega_k' = \Omega_k * a / a(t)$
5. H = surface defined by **Hill Sphere** in the SRF of the CR3BP
6. Identify  $\Omega_k' \cap H$



# EEL-1 Dispersion Manifolds: Intersections w/ Hill Sphere (SRF View)



Intersections  
with Hill Sphere

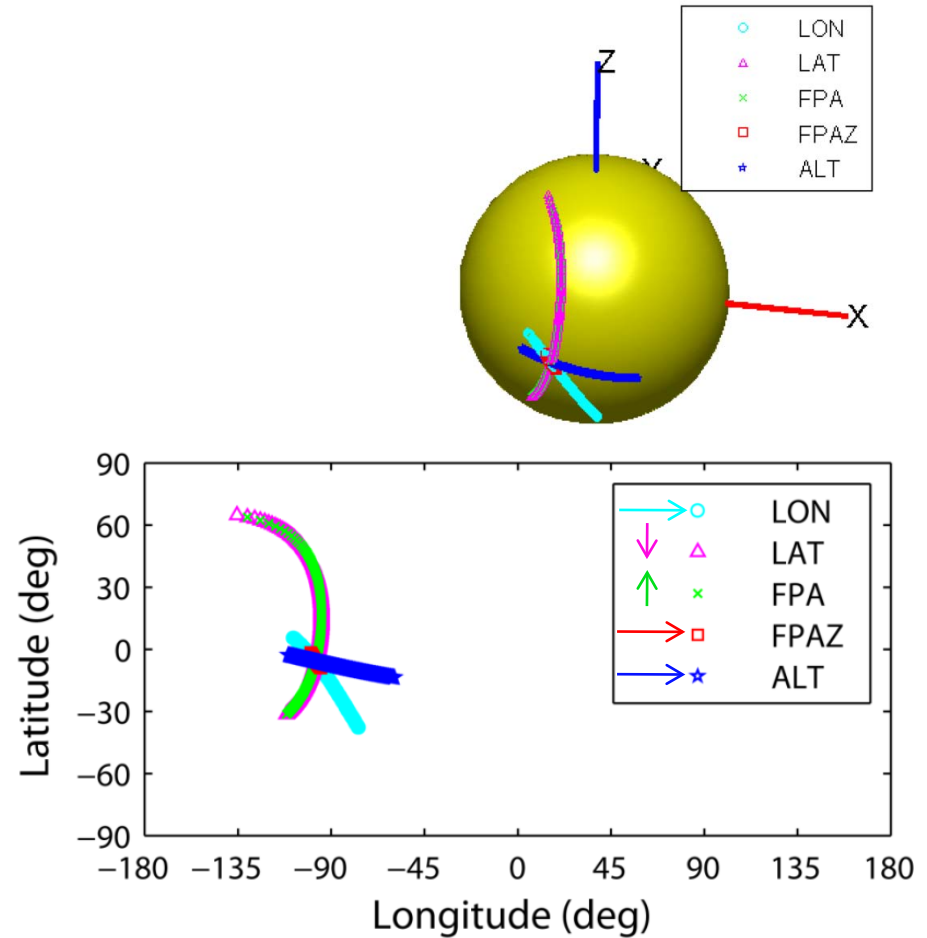
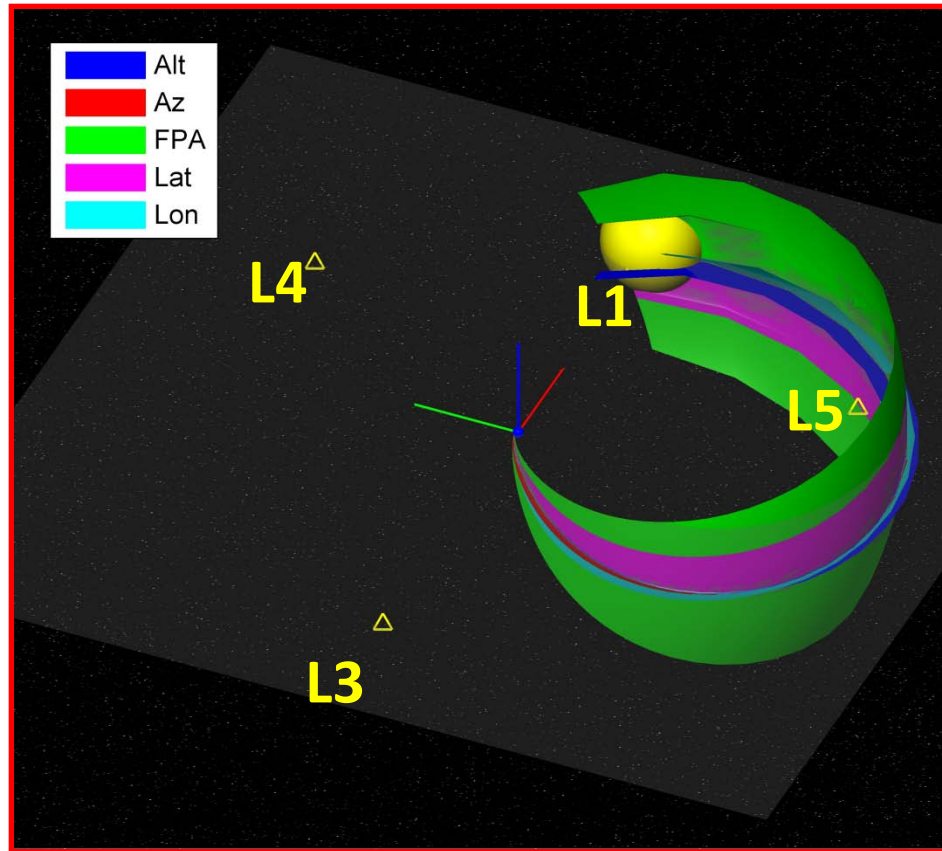


Lat/Lon of Intersections Along Hill Sphere



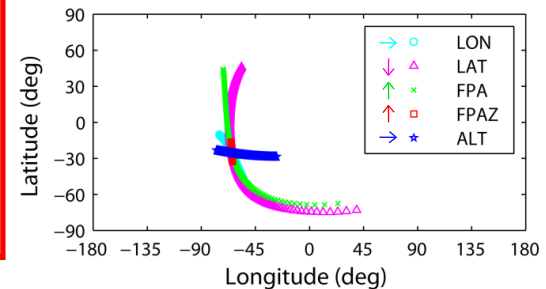
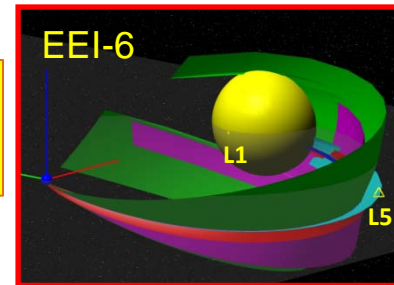
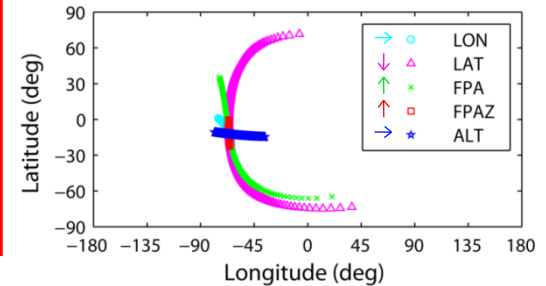
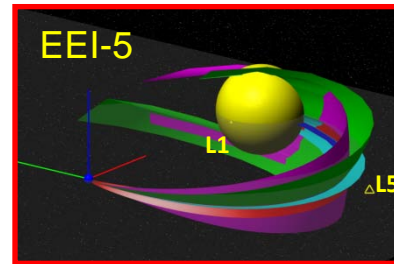
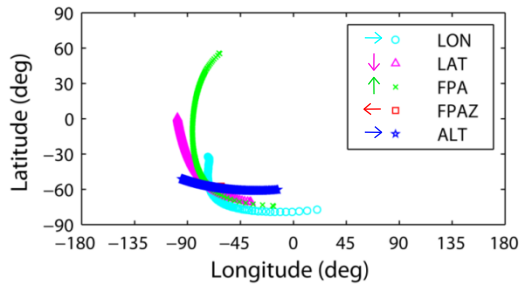
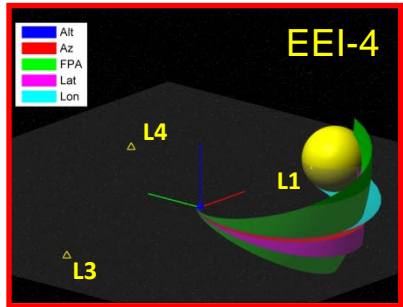
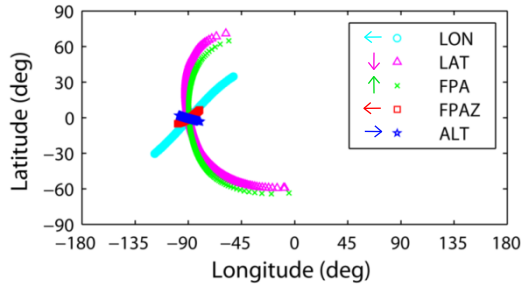
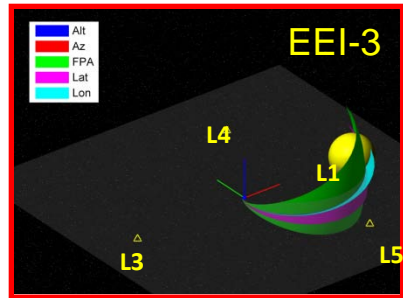


# EEL-2 Dispersion Manifolds: Intersections w/ Hill Sphere (SRF View)





# EEI-k (k=3,4,5,6) Dispersion Manifolds: Intersections w/ Hill Sphere (SRF View)



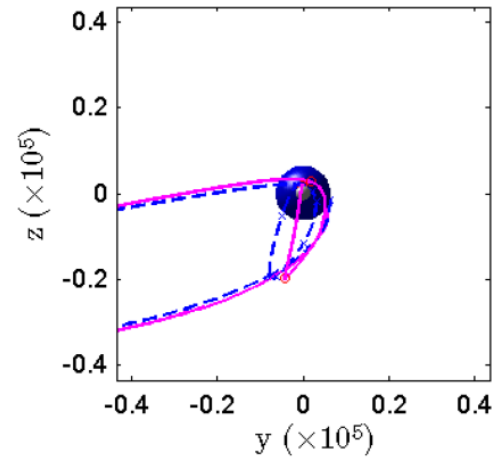
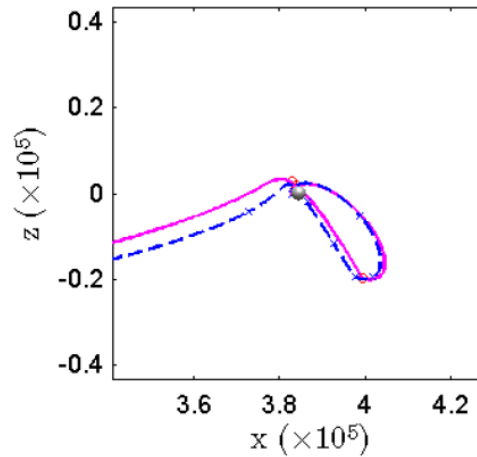
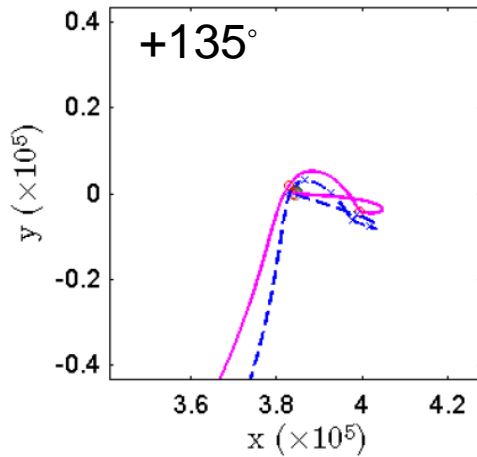
EEI Constraint Coupling Can  
Be Deduced From Hill Sphere Projections



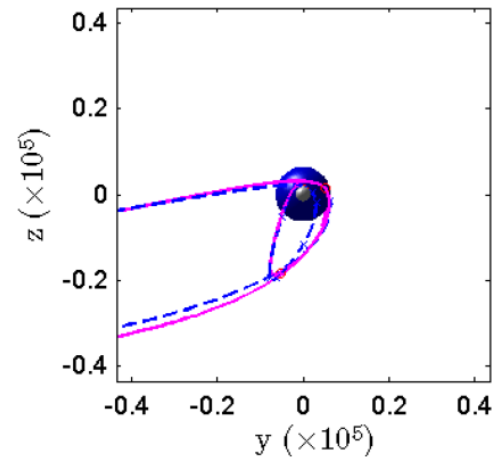
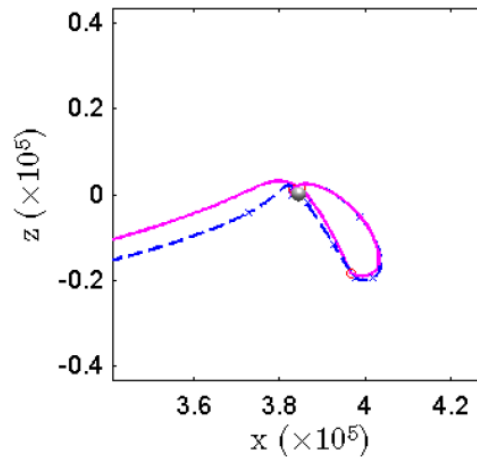
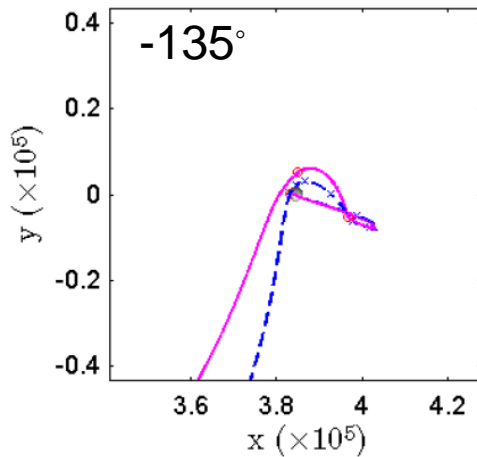
# Impact of Entry Longitude Errors

Targets: Altitude = 121.912 km, FPA = -5.86 deg,  $\Delta V = 1.5$  kps  
Initial Longitude: 76.01 deg

30 Iterations



14 Iterations

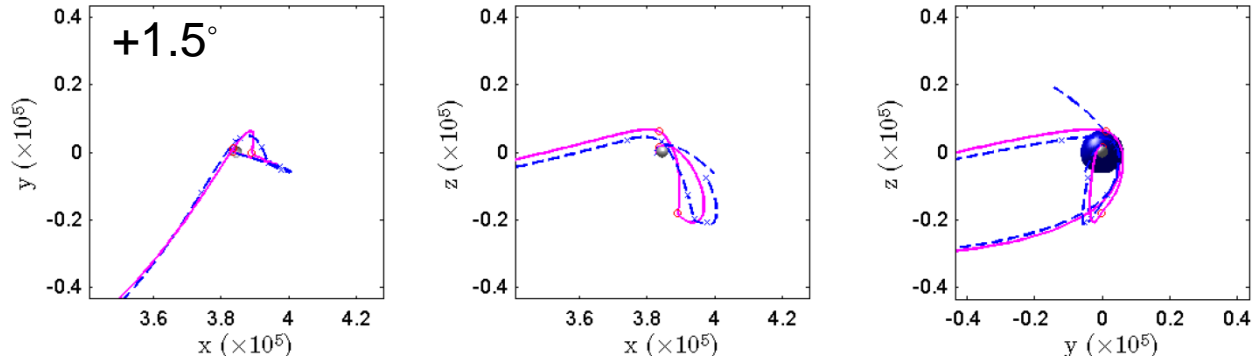




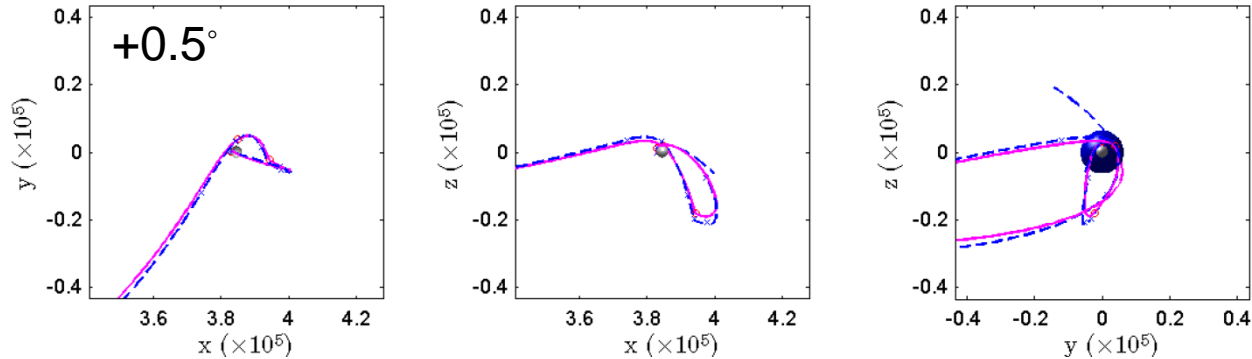
# Impact of Entry Latitude Errors

Targets: **Altitude = 121.912 km**, **FPA = -5.86 deg**,  $\Delta V = 1.5$  kps  
Initial Latitude: -1.29 deg

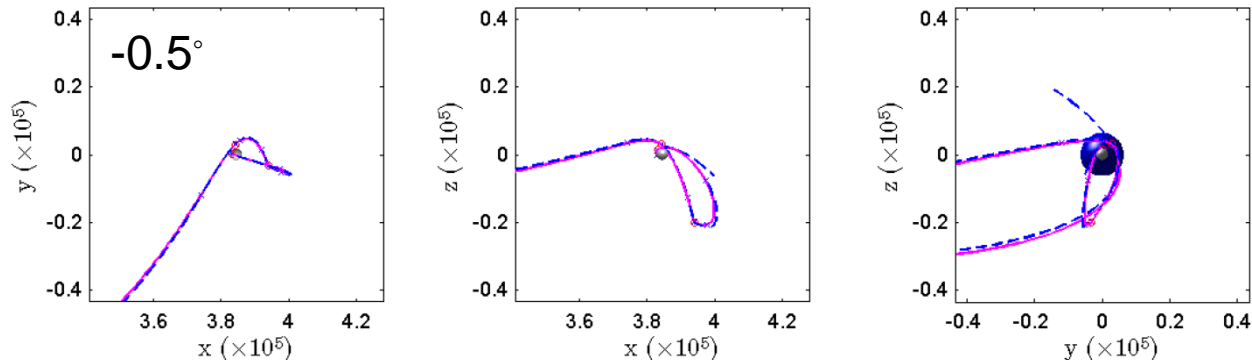
21 Iterations



10 Iterations



4 Iterations

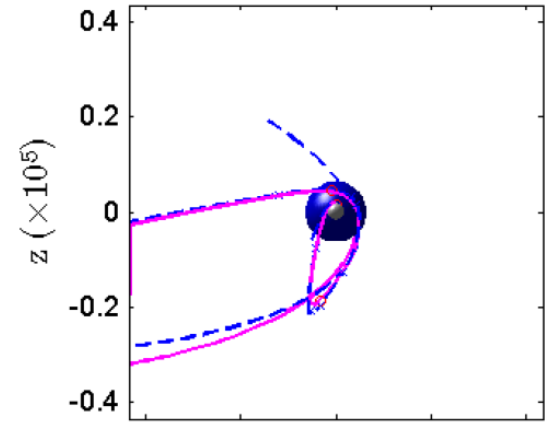
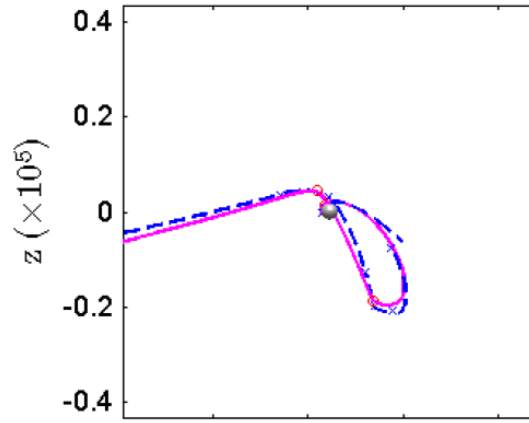
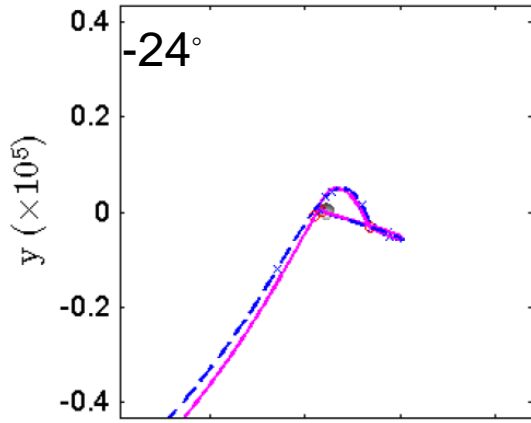




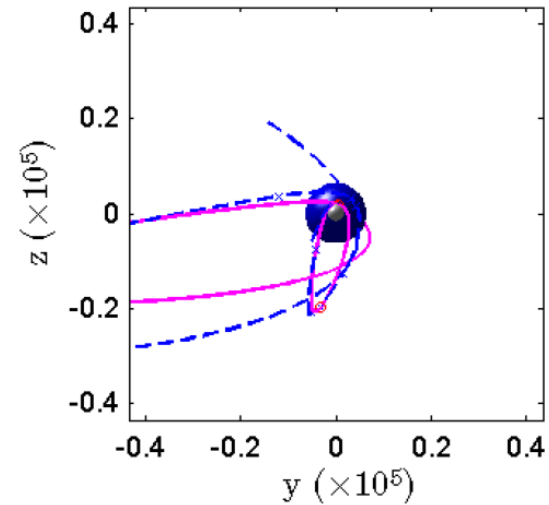
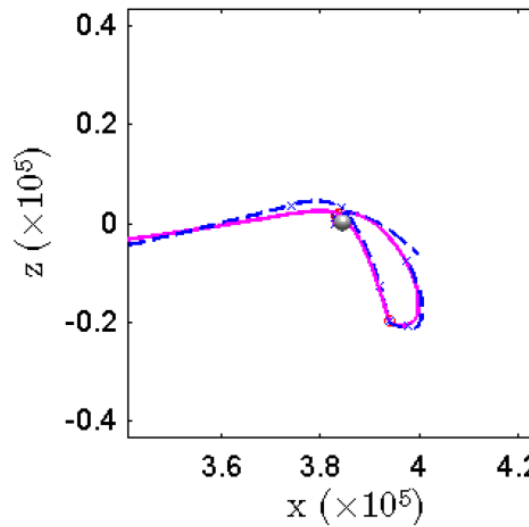
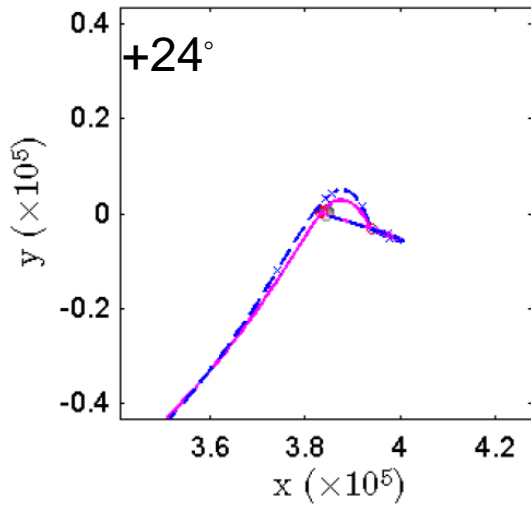
# Impact of Entry Azimuth Errors

Targets: Altitude = 121.912 km, FPA = -5.86 deg,  $\Delta V = 1.5$  kps  
Initial Azimuth = 8.41 deg

24 Iterations



8 Iterations





# Conclusions

- Without loss of generality, the precision entry problem can be studied within the context of the CR3BP and the results are easily transitioned and nearly identical to those in the EPHEM model.
- Intersections of EEI dispersion manifolds with Hill Sphere, in SRF, yields useful information regarding entry constraint coupling. This knowledge can be used in future studies to enhance startup arcs and, subsequently, targeting performance.
- Validated constraint coupling conjectures, from Hill sphere analysis, for FPA & LON, FPA & LAT, and FPA & AZ, by analyzing targeter performance in the presence of EEI errors in LON, LAT, and AZ, respectively.
- A multi-body analysis in the SRF of the Earth-Moon system offers a more representative set of startup arcs than those obtained from 2BP approximations. The resulting improved startup arcs facilitate an efficient onboard targeting process.